Electronic Supplementary Material (ESI) for Soft Matter.

Supplementary information for:

Mechano-chromic protein-polymer hybrid hydrogel to visualize mechanical strain

Masumi Taki[a,b§*], Tadahiro Yamashita[a,c§], Kazuki Yatabe[b], and Viola Vogel[a*]

a. *Laboratory of Applied Mechanobiology, Department of Health Sciences and Technology, ETH Zürich, Vladimir-Prelog-Weg 4, 8093 Zürich, Switzerland.*

b. *Department of Engineering Science, Bioscience and Technology Program, The Graduate School of Informatics and Engineering, The University of Electro-Communications (UEC), 1-5-1 Chofugaoka, Chofu, Tokyo 182-8585, Japan.*

c. *Department of System Design Engineering, Keio University, 3-14-1 Hiyoshi, Kohoku-ku, Yokohama 223-8522, Japan.*

§ These authors equally contributed to the work.

Tel: +81-42-443-5980; E-mail: taki@pc.uec.ac.jp (M.T.)

Tel: +41 44 632 08 87; E-mail: viola.vogel@hest.ethz.ch (V.V.)

Contents

1. Synthesis of Fn-FRET / PNIPAAm hydrogel

1.1. Synthesis of azido-containing PNIPAAm

As shown in Fig. S1, azido-containing poly(N-isopropylacrylamide)[1], abbreviated as azido–PNIPAAm, was synthesized and purified according to the reported procedure[2]. Briefly, its precursor co-polymerized with glycidyl methacrylate (i.e., P(NIPAAm-co-GMA)) was synthesized from commercially available monomers according to the reported procedure[3], and it was reacted with sodium azide[2] to create azido–PNIPAAm. The molar ratio of the NIPAAm / GMA or N_3 units was roughly estimated as 0.9 / 0.1 by integrating the corresponding curves of the ^{1}H NMR spectrum (Fig. S2). The number-average molecular weight (M_n) and the polydispersity of the synthesized polymer were determined to be 15 kDa and 2.6, respectively, by performing gel permeation chromatography (GPC) using polyethylene glycol (PEG) standard samples of defined molecular weights. These values are similar to the reported values (i.e., 9.2 kDa and 3.1) of the NIPAAm / GMA synthesized using the same polymerization reaction[3].

1.2. Synthesis of water-soluble crosslinker 4-arm DIB–PEG

Synthesis of the water-soluble crosslinker[4], abbreviated here as 4-arm DIB–PEG linker, is outlined in Fig. S3. DIB–ntrPhe (Carbonic acid 7,8-didehydro-1,2:5,6-dibenzocyclooctene-3-yl ester 4-nitrophenyl ester) was synthesized as described previously[5]. DIB–ntrPhe (18 μmol), poly(ethylene oxide)-4-arm-amine (4.5 μmol, commercially available from Aldrich #565733, MA, USA, average M_n 10,000), and triethylamine (4 μL) was mixed in dimethyl sulfoxide (0.35 mL), and incubated at room temperature overnight. It was purified by size-exclusion chromatography (Bio-Gel P-6 Media, exclusion limit = 6 kDa, commercially available from Bio-Rad #150-4134, Hercules, CA, USA, equilibrated with water) to obtain the pure water-soluble crosslinker (yield: 20%), which was

identified by ^{1}H NMR (Fig. S4).

The successful introduction of the dibenzocyclooctyne (DIB) moiety to poly(ethylene oxide)-4-arm-amine was also confirmed by copper-free strain-promoted azide-alkyne cycloaddition (SPAAC) reaction between the purified crosslinker and N_3–tetramethylrhodamine (N_3–TMR), which was synthesized by us previously[6]. When equivalent moles of the crosslinker and N_3–TMR were mixed together, the SPAAC reaction spontaneously occurred within several minutes. The resulting molecular weight of the TMR conjugate was above the exclusion limit (i.e., 6 kDa) of Bio-Gel P-6 Media (Fig. S5).

1.3. N-terminal azide modification of fibronectin via FXIIIa-mediated transamidation

Plasma fibronectin (Fn) in dimeric form was purified from human plasma (Zürcher Blutspendedienst SRK, Switzerland) using gelatine-sepharose chromatography as formerly described[7]. N-terminal specific azide modification of dimeric Fn catalyzed by activated blood coagulation factor XIII (FXIII) was performed according to our reported procedure[8]. Briefly, purified Fn in phosphate buffered saline (PBS) supplemented with $CaCl_2$ (2.5 mM) was mixed with an azido-containing substrate peptide (FKGGGK(N_3); abbreviated as azide; Peptide Specialty Laboratories GmbH, Heidelberg, Germany) in the presence of thrombin-activated FXIII (FXIIIa). The enzymatic reaction was conducted for 3 h at room temperature. As a negative control, a mock reaction in the absence of FXIIIa was also performed. The azide introduction by the transamidation reaction was confirmed by SPAAC reaction between Fn and DIB-TMR[6], followed by SDS-PAGE / fluorescence imaging using a conventional imager (Quantum, Vilber Lourmat, Collégien, France). A fluorescent Fn band appeared at the appropriate molecular weight only when dimeric Fn and azide was mixed in the presence of FXIIIa (Fig. 3A in the main text). Following the transamidation, azide-modified Fn (i.e., N_3–Fn) whose dimeric structure is confirmed by native PAGE analysis in our former study[8], was subjected to the next reaction in one-pot without further purification.

1.4. Fluorescence labeling of azide-modified Fn

Based on our reported procedure, N_3–Fn was doubly labeled with multiple Alexa Fluor™ 488 NHS Ester (Thermo Fisher Scientific, Molecular Probes #A20000, MA, USA) and Alexa Fluor™ 546 C_5 Maleimide (Molecular Probes #A10258) as Förster / Fluorescence resonance energy transfer (FRET) donors and acceptors, respectively (Fig. S6)[7]. Briefly, the above mixture containing N_3–Fn (0.17 nmol, final 1.0 μM) was dissolved in 50 mM $NaHCO_3$ buffer (pH 8.0) supplemented with 4 M guanidine hydrochloride (GdnHCl), mixed with Alexa 488 NHS (0.30 mM) / Alexa 546 Maleimide (0.15 mM) in one pot, and incubated for 1 hour at room temperature. The free amines of dimeric Fn were thereby randomly labeled with multiple donors, while the 4 cysteins of dimeric Fn located on the Fn type III domains, FnIII-7 and FnIII-15, were specifically labeled with acceptors (N_3–Fn-FRET). The product was separated from free dye and other impurities by size-exclusion chromatography (Bio-Gel P-100, exclusion limit = 100 kDa, commercially available from Bio-Rad #1501930, equilibrated with PBS). The purity was verified by SDS-PAGE followed by CBB staining. The band of N_3–Fn-FRET was observed using the imager (Excitation wavelength: 312 nm). The labeling ratios of donors and acceptors per dimeric Fn were determined by measuring the absorbances of N_3–Fn-FRET at 280, 498, and 556 nm (i.e., A_{280}, A_{498} and A_{556}) using NanoDrop 2000 (Thermo Fisher Scientific). The concentrations of Fn, Alexa 488-donor, and Alexa 546-acceptor fluorophores (i.e., C_{Fn}, C_D, and C_A) were then determined using the following relation:

$$\begin{pmatrix} A_{280} \\ A_{498} \\ A_{556} \end{pmatrix} = \begin{pmatrix} e_{Fn(280)} & e_{D(280)} & e_{A(280)} \\ e_{Fn(498)} & e_{D(498)} & e_{A(498)} \\ e_{Fn(556)} & e_{D(556)} & e_{A(556)} \end{pmatrix} \begin{pmatrix} C_{Fn} \\ C_D \\ C_A \end{pmatrix} \quad \text{Eq. S1}$$

where $\varepsilon_{Fn(i)}$, $\varepsilon_{D(i)}$ and $\varepsilon_{A(i)}$ represent the molar extinction coefficients of Fn, donor and acceptor at i nm, respectively. The molar extinction coefficients used for the calculation are summarized in Table S1. The average donor and acceptor labeling ratios per dimeric Fn (i.e., R_D and R_A) were determined using the following equations.

$$R_D = \frac{C_D}{C_{Fn}} \quad \text{Eq. S2}$$

$$R_A = \frac{C_A}{C_{Fn}} \quad \text{Eq. S3}$$

Consequently, we obtained 5.7 donors and 4.2 acceptors per dimeric N_3–Fn-FRET, and 7.3 donors and 3.3 acceptors per dimeric Fn-FRET.

Due to the random labeling of amino groups with Alexa 488, the resulting Fn-FRET shows slightly different batch-to-batch responses to mechanical stretch, or denaturation in solution[7]. In the whole experiments of this report, we thus used a single batch of N_3–Fn-FRET and a non-azidated Fn-FRET as a control. The FRET shifts with regard to their conformational changes were all characterized by a denaturation assay as used previously[7, 17] and described below in section 2.1.

We alternatively attempted to construct N_3–Fn-FRET in two different ways. (1) Guinea pig transglutaminase (gpTGase, commercially available from Sigma #T5398)-mediated transamidation instead of FXIIIa toward native Fn was used to introduce azide group into Fn. (2) Fluorescence labeling of native dimeric Fn was carried out following N-terminal azide introduction of Fn-FRET by FXIIIa-mediated transamidation. In both cases, Fn showed random aggregation of during the transamidation and N_3–Fn-FRET could not be obtained successfully (data not shown; summarized in Fig. S6).

1.5. Preparation of dimeric Fn-FRET hydrogels on PDMS sheets

The Fn-FRET-conjugated hydrogel (i.e., Fn-FRET / PNIPAAm) was prepared on a polydimethylsiloxane (PDMS) sheet according to the reaction procedure summarized in Fig. S7. First, acetone precipitation of the above N_3-conjugated Fn-FRET (6 pmol) was performed, and the deposit was dissolved in 2 μL of PBS containing 1 M GdnHCl and 10 mM water-soluble crosslinker (i.e., 20 nmol of 4-arm DIB–PEG linker). It was incubated at room temperature for 1 hour in a microtube, to make sure that the azide group of N_3–Fn-FRET efficiently form covalent bonds with the crosslinker by SPAAC reaction. After removal of the insoluble fraction by brief centrifugation, the supernatant

(2 μL) was mixed with 2 μL of 2 mM aqueous solution of azido–PNIPAAm (4 nmol) on ice. The solution was immediately spotted on a PDMS sheet and incubated for at least 4 hours on ice. The solidified hydrogel droplets were washed with PBS three times. As a control, the hydrogel droplets were additionally incubated with 1 mM dithiothreitol (DTT) for 1 hour at room temperature to cleave the dimeric Fn by reducing the disulfide bonds.

In addition, two negative controls were prepared by forming hydrogels using N_3-capped Fn-FRET or non-azidated Fn-FRET[7] instead of N_3–Fn-FRET following the same protocol. The N_3-capped Fn-FRET was obtained by incubating the N_3–Fn-FRET (6 pmol) noted above with DIB–biotin[6] (referred as a DIB modifier in the body text; 11 nmol, 1.7 mM) in PBS for 2 hours at room temperature. Non-azidated Fn-FRET was obtained by labeling the native human plasma Fn with the donor and acceptor fluorophores as described above.

2. FRET analysis of N_3–Fn-FRET and Fn-FRET / PNIPAAm hydrogels

2.1. Denaturation assay of N_3–Fn-FRET probe

The conformational change of N_3–Fn-FRET was evaluated compared to the calibrated Fn-FRET signals under the presence of different denaturant concentrations. While our labeling approach does not allow to calculate exact donor-acceptor distances, it is well suited to probe and visualize a wide range of fibronectin conformations. We have used this FRET-labeling approach extensively in the lab and obtained highly valuable and meaningful results as evidenced by numerous publications[10-23]. To validate that conformational changes of N_3–Fn-FRET can be induced, we denatured N_3–Fn-FRET by GdnHCl as described previously[7]. Briefly, a glass coverslip was immersed in 2% bovine serum albumin (BSA) solution in water for 30 minutes at room temperature to passivate the surface. After drying the surface of the coverslip, 2 μL of N_3–Fn-FRET solutions containing GdnHCl, ranging from 0 to 4 M were spotted. Then, the Fn-FRET ratios from the hydrogels were measured as described below. Non-azidated Fn-FRET was also tested following the same protocol (Fig. S8).

2.2. Stretching of Fn-FRET hybrid hydrogels on PDMS sheets

For our proof-of-concept studies, the hydrogel droplets formed on the PDMS sheets were exposed to uniaxial stretch using a stretching device (Fig. S9A); the PDMS sheet was designed so that the hydrogels positioned at the center were uniaxially stretched[24]. It was set on the stretching chamber with both the side edges immobilized by metal bars and screws (Fig. S9B). The initial length of the PDMS sheet was set at 4 cm and it was then stretched to 15 cm by extending the chamber by screwing the bar in the center (Fig. S9C). The PDMS sheets, either with or without getting stretched, were transferred to a metal holder keeping the stretching level (Fig. S9D) for confocal microscopy.

To roughly estimate strain of the hydrogel droplet imposed by stretching the PDMS sheet, the following experiment using fluorescently-colored hydrogel droplets was performed. The hydrogel for strain test was synthesized using 2 μL of 6 μM N_3–TMR in DMSO (12 pmol) instead of N_3–Fn-FRET (6 pmol), according to the protocol described in section 1.5. We assume that the incorporation of Fn-FRET molecules does not dramatically change the elastic property of the material as used in this control, because the percentage of N_3–Fn-FRET in the hydrogel is less than 0.03% (molar fraction in the hydrogel components), or less than 1% in total mass. For this control, the TMR / PNIPAAm hydrogel droplets were formed on the PDMS sheet mounted on the stretching chamber. The PDMS sheet was then stretched from 4 cm to 15 cm. The fluorescence imaging before and after stretching the PDMS sheet were performed by using a conventional fluorescent gel imager (Gel Doc XRS+; Bio-Rad) (Fig. S10A and B). The longitudinal and orthogonal lengths of the initial and stretched droplets to the stretching direction were evaluated using ImageJ software (National Institute of Health; NIH, MD, USA). The hydrogel strain ε_H in both directions was quantified according to

$$\varepsilon_H = \frac{L - L_0}{L_0} \qquad \text{Eq. S4}$$

where L_0 and L represent the droplet length before and after stretching the PDMS sheet, respectively. The measured hydrogel strain along the stretching direction was 90%, while 15% of the orthogonal compressive strain was observed (Fig. S10C). This suggests that the PDMS strain of 275% was not completely transferred to the hydrogel droplets during the stretching procedure, because there was no covalent bonding between PDMS and hydrogel in our system.

2.3. Observation of Fn-FRET hybrid hydrogels using confocal microscopy

The FRET ratios of N_3–Fn-FRET in solution or of Fn-FRET / PNIPAAm hydrogels were recorded using a confocal laser scanning microscope (FV1000, Olympus, Tokyo, Japan) with a 10x objective lens (N.A. 0.40). Either the BSA-coated coverslip with N_3–Fn-FRET solution droplets, or the PDMS sheet with Fn-FRET / PNIPAAm hydrogel

hybrid hydrogels were placed on the stage of the confocal microscope under the defined PDMS strains. The samples were excited at 488 nm and the donor and the acceptor emission images were obtained at 510–530 nm and 560–580 nm, respectively. During the acquisition of both image channels, the excitation intensity was kept the same and the emission was collected using the same photo-multiplier operated at the same voltage. Kalman filter (3 times, line mode) was used to reduce the fluctuation of the dark current. To avoid artifacts from the hydrogel-PDMS and hydrogel-air interface, the focal point was set at least 50 μm above the PDMS surface and 50 μm below the hydrogel top (Fig. S11A and B). Control images from regions that did not contain the hydrogel sample were taken under otherwise the same conditions. Alexa 488 solution was also observed to evaluate the crosstalk factor of the emission light of the donor fluorophore to the acceptor channel.

2.4. Image processing

The obtained images were processed using MATLAB (2016b, Mathworks, MA, USA). First of all, all images were processed using a 3 x 3 mean filter to remove noise fluctuations and the mean dark current intensity calculated from a blank image was then subtracted from all pixels.

The region of interest (ROI) to evaluate pixel-by-pixel FRET ratios was selected from each FRET image in an objective and reproducible way. The hydrogel region in the image was first extracted by adjusting the contrast followed by thresholding: the contrast of the donor and acceptor images was tuned using “imadjust” function of MATLAB, which optimizes the image contrast so that the bottom 1% and the top 1% of the resulting image pixels turn zero and saturate, respectively. From the contrast-tuned donor and acceptor images, the area where the pixel intensity is higher than 10% of the maximum value in both channels was counted as the hydrogel region. Then, the area where the pixels contain saturating values either in the donor or the acceptor images was removed from the hydrogel region. The remaining area was defined as ROI, where pixel-by-pixel FRET ratios were evaluated in the following calculation. Note that these

contrast-tuned donor and acceptor images were only used to define ROI. For calculation of FRET ratios, donor and acceptor images without tuning the contrast were used in the following processes.

Next, the background intensities i_{0D} and i_{0A} in both donor and acceptor channels, respectively, were determined by evaluating all pixel intensities contained in the control images. Then, a pair of donor and acceptor images of an Alexa 488 solution was analyzed to determine the cross-talk factor C. The cross-talk at each pixel C_{ij} was calculated by processing the donor and the acceptor images of the Alexa 488 solution as follows.

$$C_{ij} = \frac{I_{A488ij} - i_{0A}}{I_{D488ij} - i_{0D}} \qquad \text{Eq. S5}$$

where I_{D488ij} and I_{A488ij} represent the intensities of the corresponding pixels of the images of the Alexa 488 solution in the donor and the acceptor channels, respectively. Then, the mean of C_{ij} was used as the cross-talk factor C. The FRET ratios of the individual pixels r_{ij} of the hydrogel images were calculated using the following equation.

$$r_{ij} = \frac{I_{Aij} - i_{0A} - C\left(I_{Dij} - i_{0D}\right)}{I_{Dij} - i_{0D}} \qquad \text{Eq. S6}$$

where I_{Dij} and I_{Aij} represent the intensity of the corresponding pixels of the paired donor and acceptor images, respectively. In the end, a set of FRET ratios r_{ij} in the ROI was obtained. A pair of donor and acceptor images was analyzed to obtain a set of r_{ij} and the median value was used as the representative information of the microscopic sight for further analysis. Thus, each FRET data point shown in all of the figures represents the median of FRET ratios in the ROI of each individual microscopic FRET image.

2.5. Statistical analysis

The median FRET ratios in the ROI observed from the hydrogels under defined strains were analyzed using two-tailed Welch's *t*-test with Excel 2011 (Microsoft,

Redmond, WA, USA). A *p* value less than 0.05 was considered statistically significant. The results of all *p* values are shown in Table S2.

2.6. Detailed description of strained Fn-FRET hybrid hydrogels

The FRET images of Fn-FRET / PNIPAAm hydrogels, either relaxed or stretched, were compared in Fig. S12A and B. The FRET ratio dropped by stretching the PDMS sheet. During the stretch, one of the hydrogel droplets spontaneously detached from the PDMS sheet. The FRET ratio of this detached hydrogel droplet was the same as that observed under relaxation (Fig. S12C). When the Fn-FRET / PNIPAAm hydrogels treated with DTT was stretched, they cracked into pieces and the FRET value raised to the same level as that of non-treated Fn-FRET / PNIPAAm hydrogel under relaxation (Fig. S12D). This suggests that the dimeric Fn was cleaved by DTT and that the mechanical defects subsequently propagated by stress concentration when stretched, resulting in the random rupture of the whole hydrogel droplet.

Throughout the experiment, the hydrogel droplet did not crack unless treated with DTT. Although the detachment of the hydrogel from the PDMS sheet is a technical limitation of this measurement system, the hydrogel itself had enough mechanical strength to keep the integrity under the strain.

3. Supplementary figure

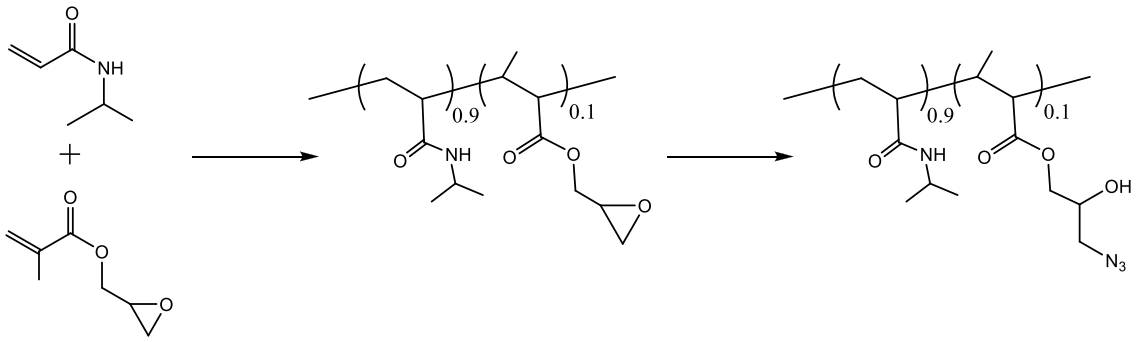

Fig. S1. Synthesis of P(NIPAAm-co-GMA) and azido–PNIPAAm. The former was synthesized from commercially available monomers (i.e., NIPAAm and GMA), and it was reacted with sodium azide to afford the latter. The molar ratio of NIPAAm / GMA or N_3 unit was estimated as 0.9 / 0.1 by ^{1}H NMR spectra.

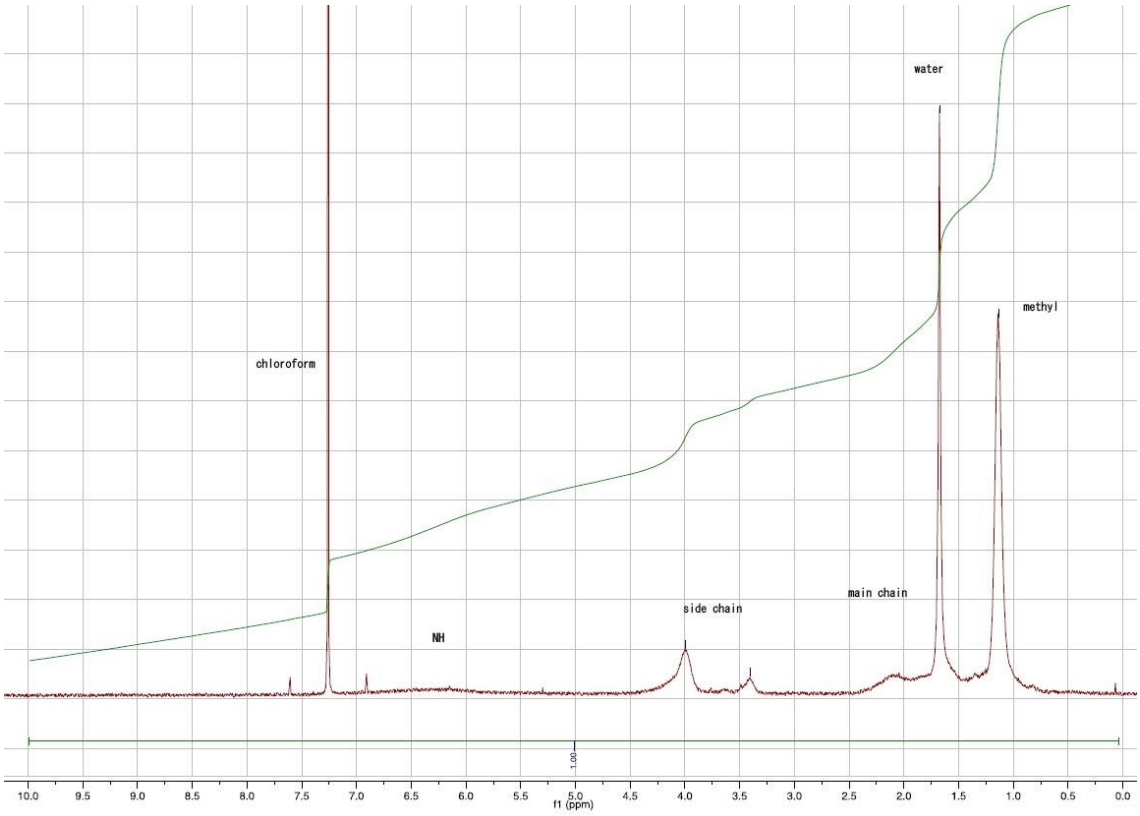

Fig. S2. ^{1}H NMR spectrum of purified azido–PNIPAAm in $CDCl_3$. Note that epoxy protons of the precursor (i.e., P(NIPAAm-co-GMA)) around 2.7 – 3.0 ppm completely disappeared[2].

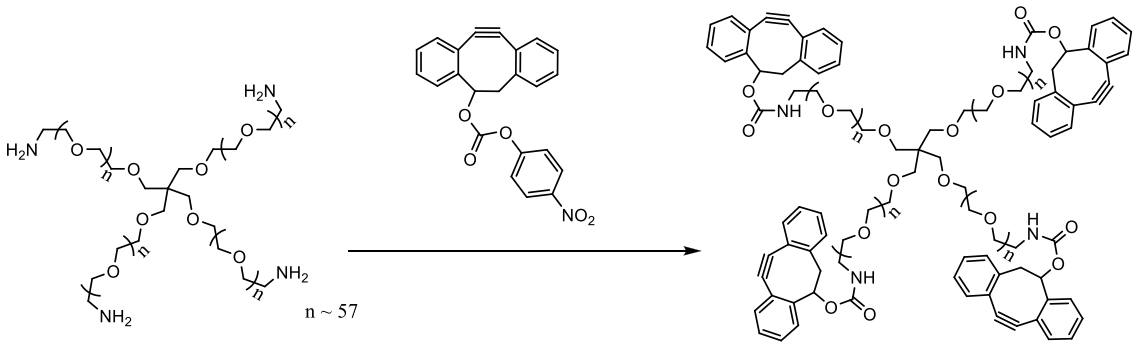

Fig. S3. Synthesis of the water-soluble crosslinker (i.e., 4-arm DIB–PEG linker). Carbonic acid 7,8-didehydro-1,2:5,6-dibenzocyclooctene-3-yl ester 4-nitrophenyl ester (i.e., DIB–ntrPhe) and poly(ethylene oxide)-4-arm-amine was coupled in the presence of triethylamine as a base, to afford the desired crosslinker for the click chemistry.

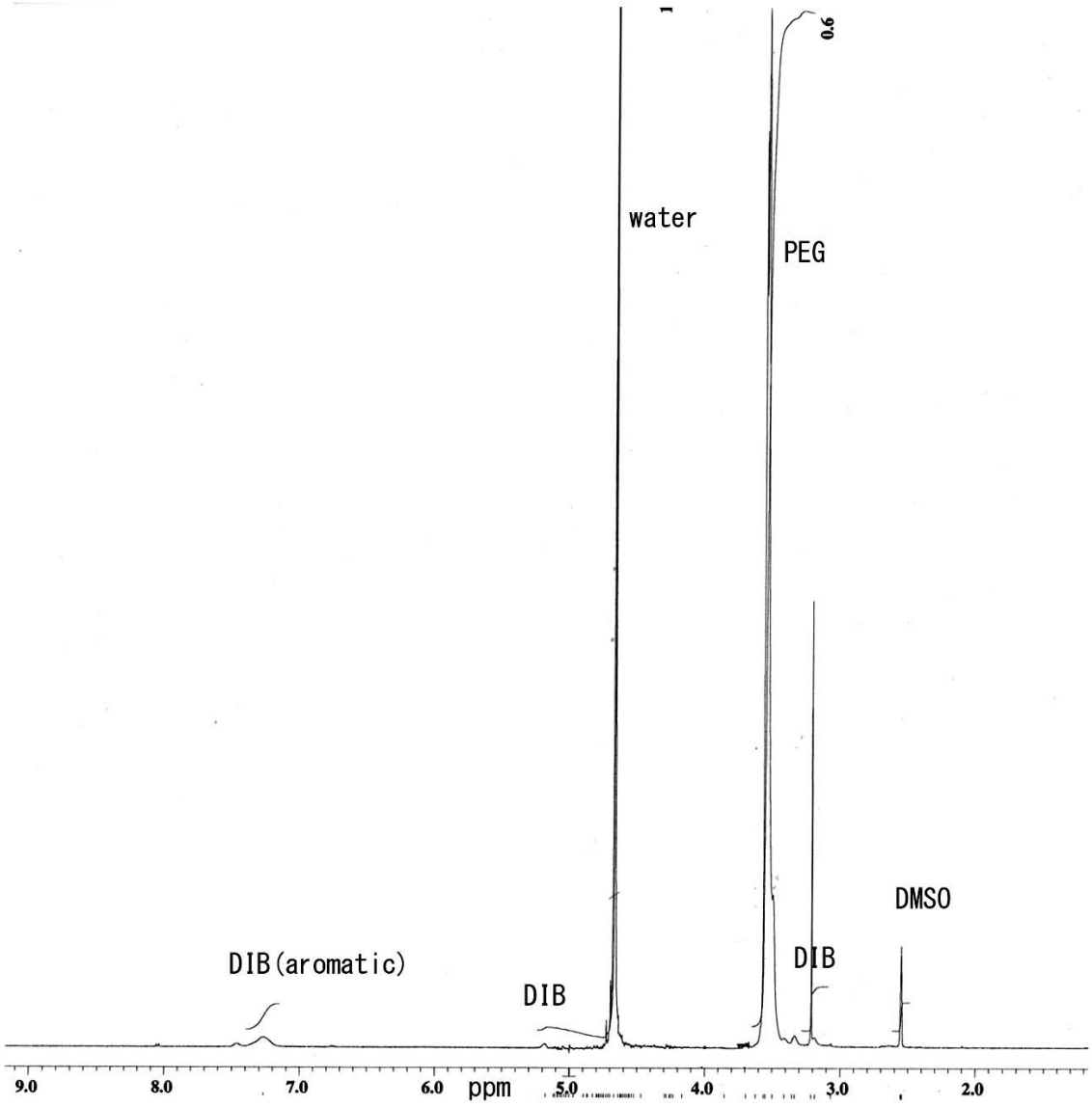

Fig. S4. ^{1}H NMR spectrum of purified water-soluble crosslinker (i.e., 4-arm DIB–PEG linker) in D_2O.

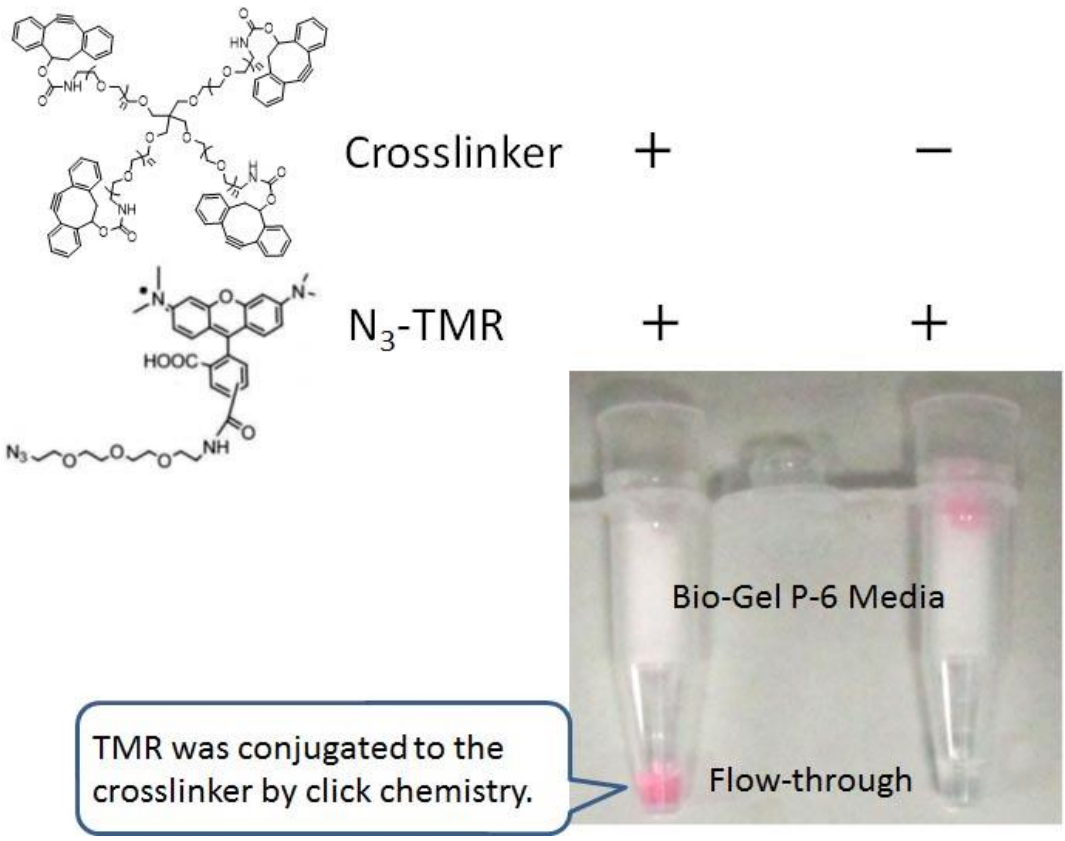

Fig. S5. SPAAC reaction between the purified crosslinker and N_3–TMR. Because the molecular weight of the tetramethylrhodamine (TMR)-conjugated crosslinker was around 11 kDa, which is above the exclusion limit of Bio-Gel P-6 Media, the red fluorescence went to the flow-through fraction.

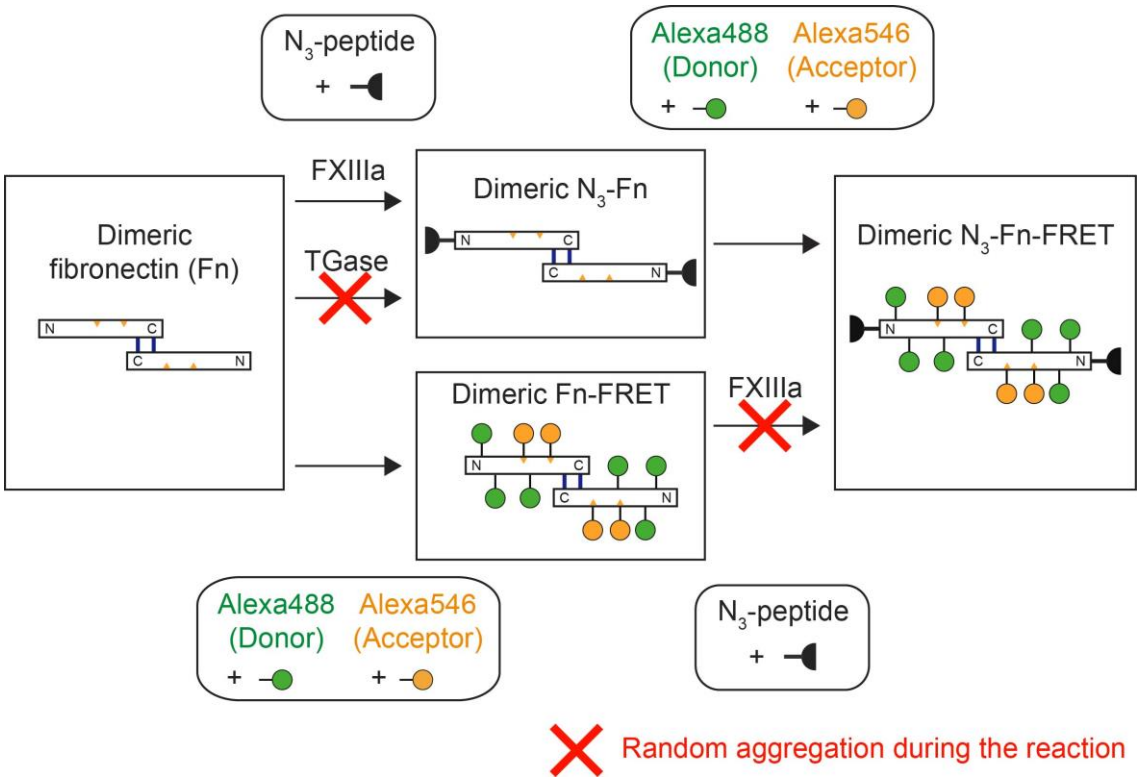

Fig. S6. Several construction strategies for obtaining N_3-conjugated Fn-FRET were explored. Guinea pig transglutaminase (gpTGase)-mediated transamidation toward native dimeric Fn or FXIIIa-mediated one toward non-azidated Fn-FRET resulted in random aggregation. Therefore, dimeric Fn was first modified with N_3–peptide using FXIIIa followed by FRET labeling throughout this study.

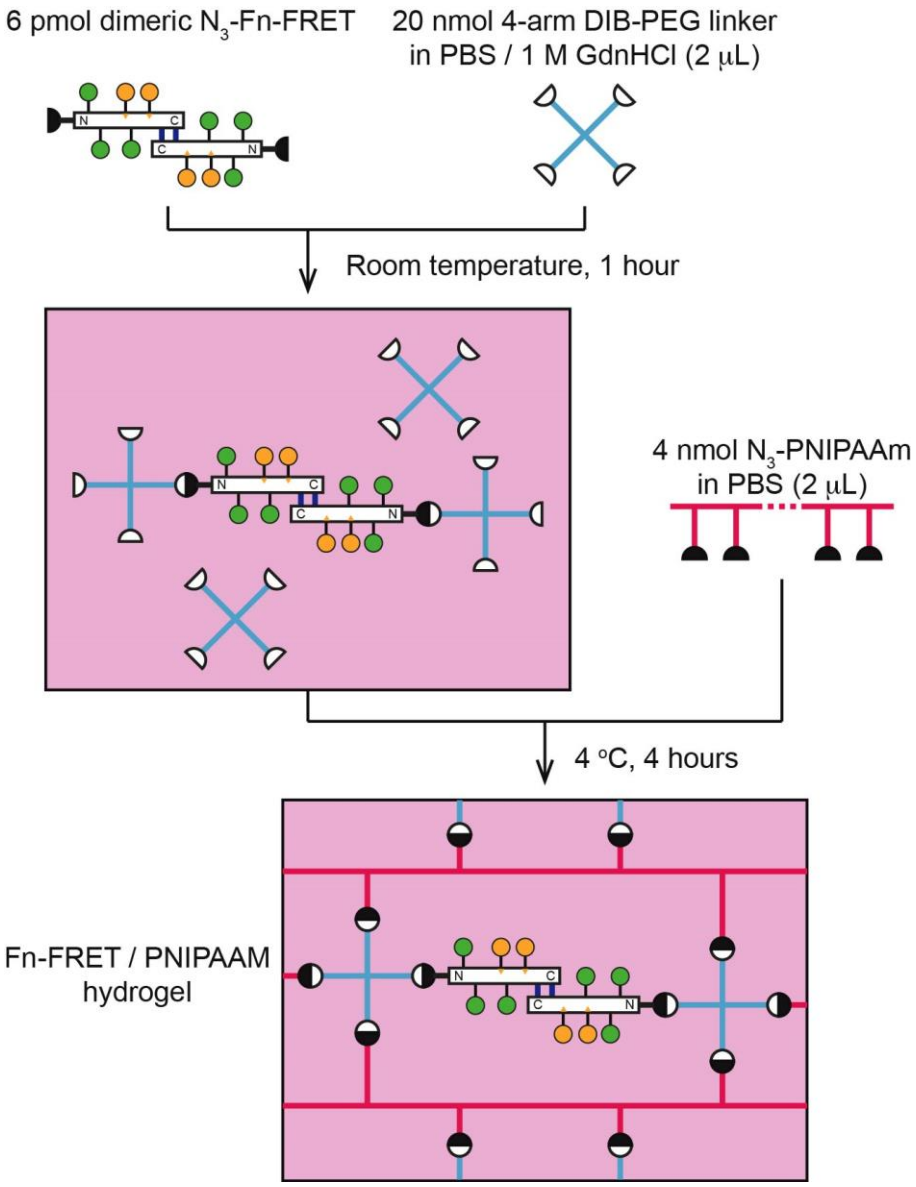

Fig. S7. Synthesis of the successfully implemented Fn-FRET-conjugated hydrogel protocol. N_3-conjugated Fn-FRET, partially denatured by 1 M GdnHCl / PBS, was conjugated with excess amount of 4-arm DIB–PEG linker by SPAAC reaction. Then, it was successively mixed with N_3–PNIPAAm on a PDMS sheet, to form the solidified hydrogel droplets.

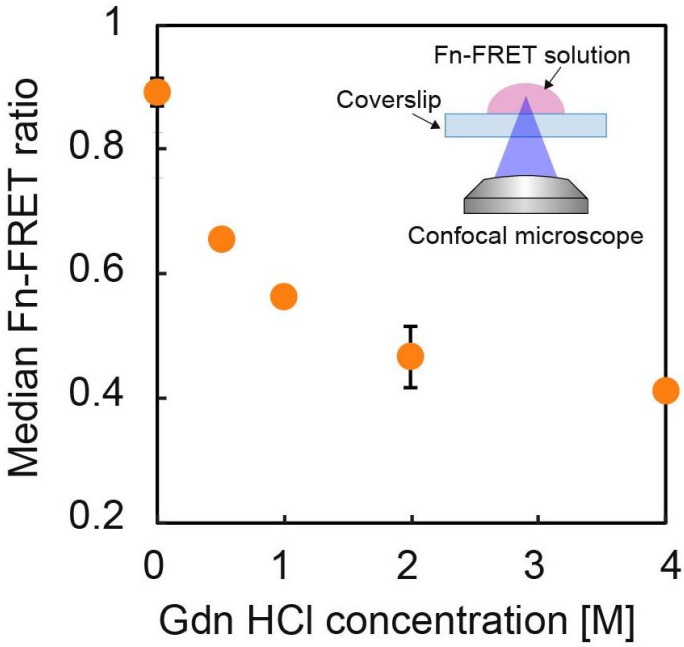

Fig. S8. Denaturation curve of Fn-FRET without azido group in solution under increasing concentrations of GdnHCl.

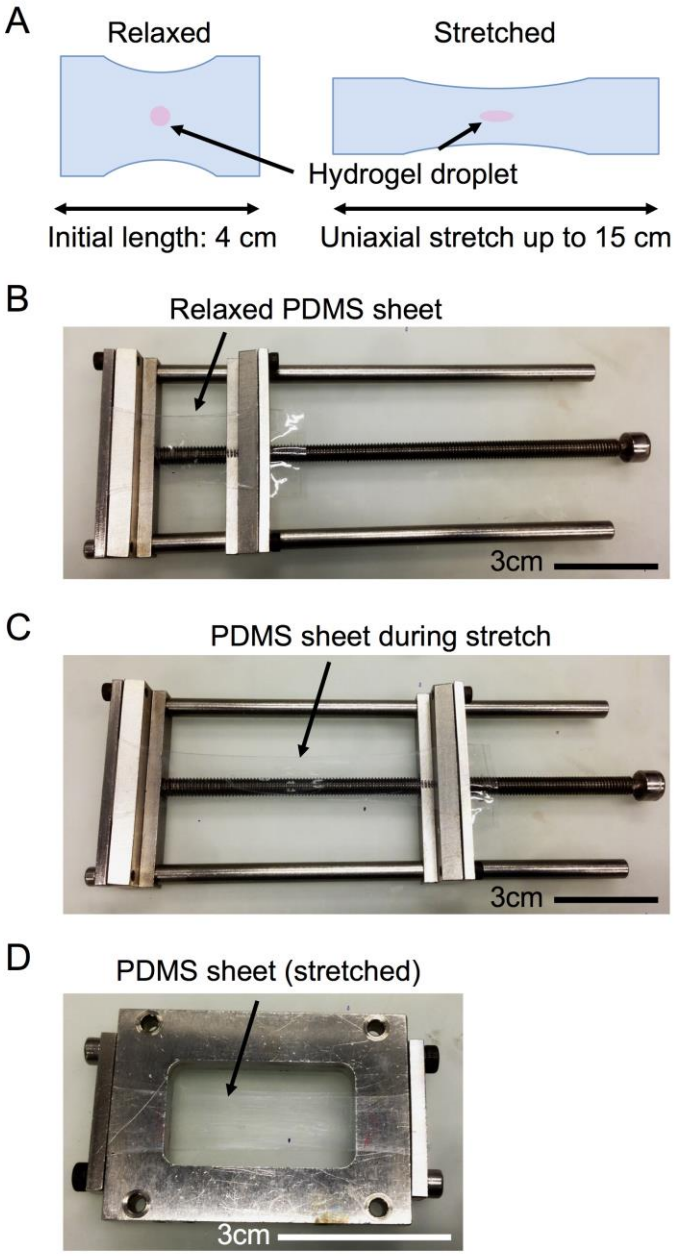

Fig. S9. The stretch assay consisting of a stretching device and a metal holder. (A) Schematic representation of the assay. The PDMS sheet was uniaxially stretched from 4 cm to 15 cm. (B) A PDMS sheet with hydrogel droplets was placed in the stretching chamber. The initial length of PDMS sheet between the metal bars is defined as L_0. (C) The PDMS sheet was stretched by screwing the metal bar in the middle. L represents the PDMS sheet length. (D) The PDMS sheet was transferred to a metal holder keeping the strain constant during confocal microscopy.

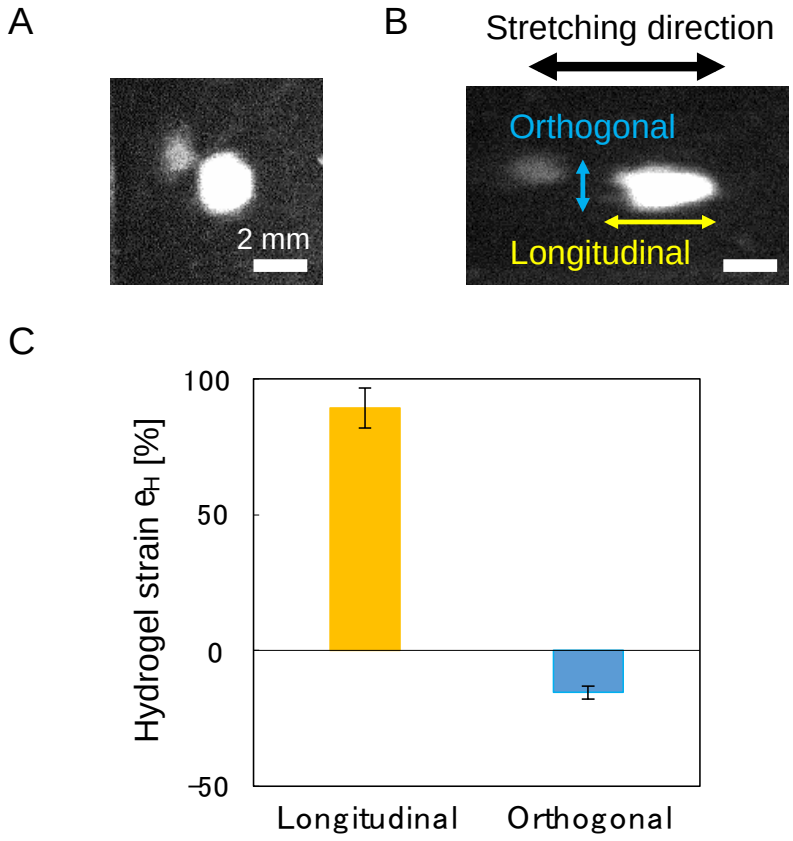

Fig. S10. Assessment of the TMR / PNIPAAm hydrogel droplet strain ε_H as the PDMS sheet gets stretched. (A) Fluorescence image of TMR / PNIPAAm hydrogel droplet without straining the PDMS sheet (PDMS sheet length: 4 cm). (B) Fluorescence image of the stretched TMR / PNIPAAm hydrogel droplet (PDMS sheet length: 15 cm; +275% PDMS strain). (C) Hydrogel droplet strains ε_H longitudinal and orthogonal to the stretching direction. The error bars represent the standard deviations of five different droplets.

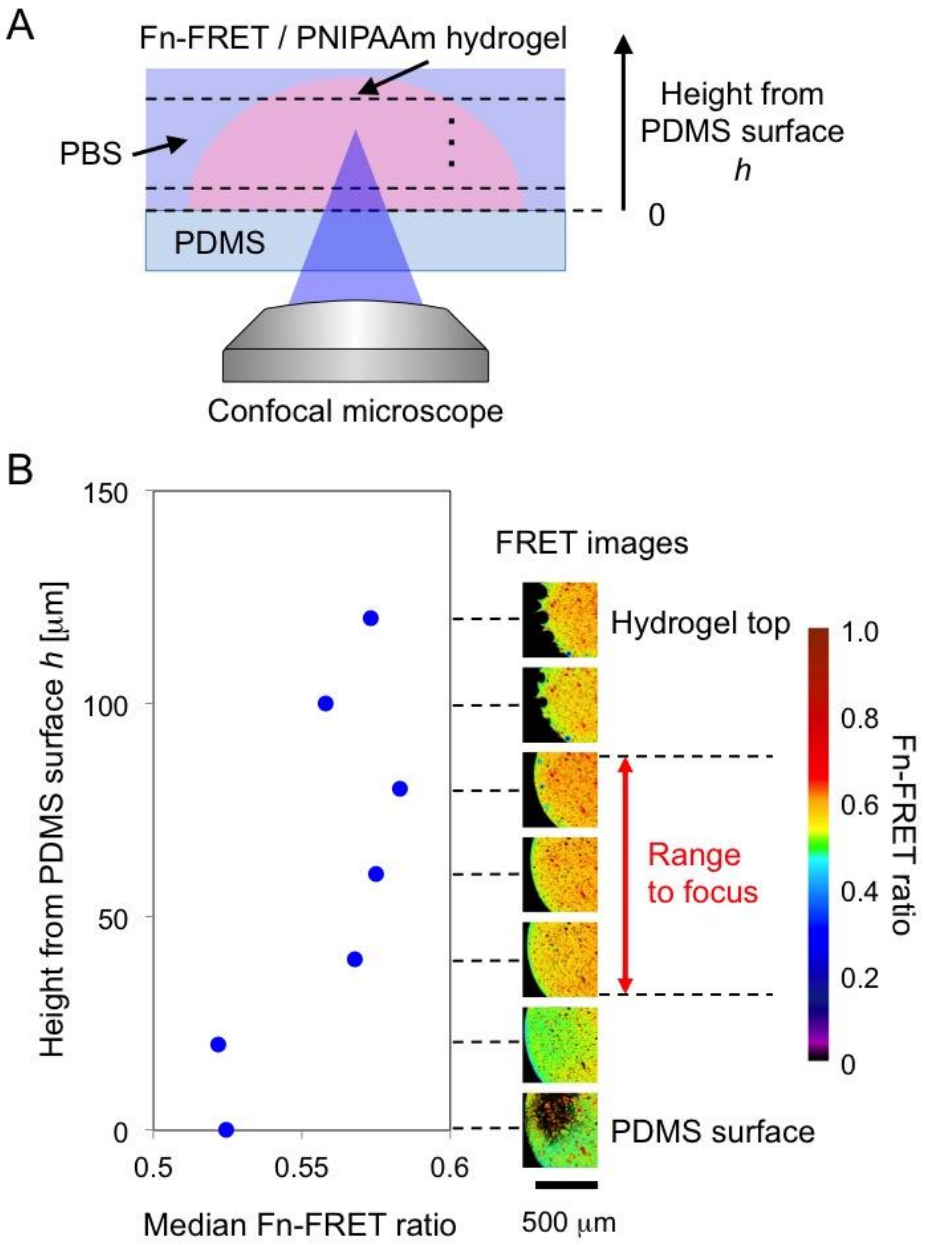

Fig. S11. Determination of focus height during confocal microscopy. (A) FRET was observed while changing the height of the focal point. (B) Comparison of Fn-FRET ratios observed at the different height of the same hydrogel droplet. Throughout this work, we report the FRET ratios observed when focusing around the middle height of the hydrogel droplets.

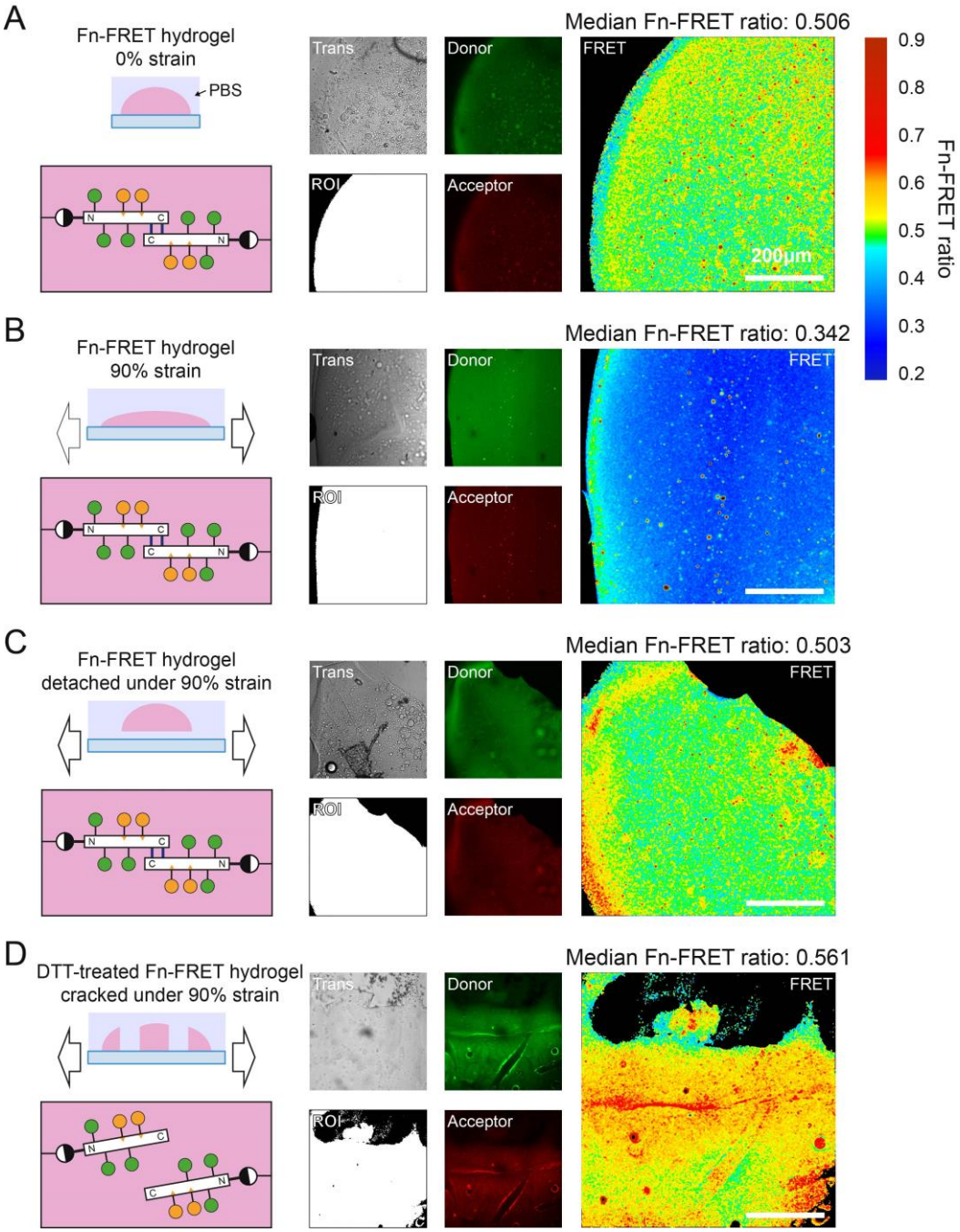

Fig. S12. Comparison of FRET images of Fn-FRET / PNIPAAm hydrogel under different conditions. (A) FRET image of N_3–Fn-FRET / PNIPAAm hydrogel without strain. (B) FRET image of N_3–Fn-FRET / PNIPAAm hydrogel at 90% strain. (C) FRET image of N_3–Fn-FRET / PNIPAAm hydrogel when detached during the stretching from the PDMS sheet. (D) FRET image of N_3–Fn-FRET / PNIPAAm hydrogel treated with DTT at 90% strain. The hydrogel cracked into pieces during the stretching.

4. Supplementary table

Table S1. Molar extinction coefficients ε [M^{-1} cm^{-1}] used to determine labeling ratios.

Substance	280 nm	498 nm	556 nm
Fibronectin[9]	563,200	0	0
Alexa 488 (donor)	8,790	71,000	0
Alexa 546 (acceptor)	72,500	13,000	104,000

Table S2. *p* values of statistical tests related to Fig. 4D.

Sample (Compared levels of strain)	*p* value	Corresponding plots
N_3–Fn-FRET (0% v.s. 90%)	0.000238	Blue (closed v.s. open)
N_3–Fn-FRET treated with DTT (0% v.s. 90%)	0.453	Green (closed v.s. open)
Capped N_3–Fn-FRET (0% v.s. 90%)	0.488	Red (closed v.s. open)
Fn-FRET (0% v.s. 90%)	0.307	Brown (closed v.s. open)

Two-tailed Welch's *t*-test

5. References

1. J. Q. Wang, Z. Y. Kang, B. Qi, Q. S. Zhou, S. Y. Xiao and Z. Q. Shao, *RSC Adv.*, 2014, **4**, 51510-51518.
2. J. Q. Wang, Z. T. Zhang, Y. H. Liu, Y. X. Lv and Z. Q. Shao, *Int. J. Polym. Mater. Polym. Biomater.*, 2015, **64**, 104-110.
3. A. K. Ekenseair, K. W. M. Boere, S. N. Tzouanas, T. N. Vo, F. K. Kasper and A. G. Mikos, *Biomacromolecules*, 2012, **13**, 1908-1915.
4. K. Barker, S. K. Rastogi, J. Dominguez, T. Cantu, W. Brittain, J. Irvin and T. Betancourt, *J. Biomater. Sci. Polym. Ed.*, 2016, **27**, 22-39.
5. X. Ning, J. Guo, M. A. Wolfert and G. J. Boons, *Angew. Chem., Int. Ed.*, 2008, **47**, 2253-2255.
6. K. Ebisu, H. Tateno, H. Kuroiwa, K. Kawakami, M. Ikeuchi, J. Hirabayashi, M. Sisido and M. Taki, *ChemBioChem*, 2009, **10**, 2460-2464.
7. M. L. Smith, D. Gourdon, W. C. Little, K. E. Kubow, R. A. Eguiluz, S. Luna-Morris and V. Vogel, *PLoS Biol.*, 2007, **5**, 2243-2254.
8. S. M. Fruh, P. R. Spycher, M. Mitsi, M. A. Burkhardt, V. Vogel and I. Schoen, *ChemBioChem*, 2014, **15**, 1481-1486.
9. E. P. Gee, D. Yuksel, C. M. Stultz and D. E. Ingber, *J. Biol. Chem.*, 2013, **288**, 21329-21340.
10. B. J. Li, Z. Lin, M. Mitsi, Y. Zhang and V. Vogel, *Biomater. Sci.*, 2015, **3**, 73-84.
11. W. R. Legant, C. S. Chen and V. Vogel, *Integr. Biol.*, 2012, **4**, 1164-1174.
12. L. A. Touryan, G. Baneyx and V. Vogel, *Colloids Surf. B Biointerfaces*, 2009, **74**, 401-409.
13. K. E. Kubow, E. Klotzsch, M. L. Smith, D. Gourdon, W. C. Little and V. Vogel, *Integr. Biol.*, 2009, **1**, 635-648.
14. M. Antia, G. Baneyx, K. E. Kubow and V. Vogel, *Faraday Discussions*, 2008, **139**, 229-249.
15. L. Baugh and V. Vogel, *J. Biomed. Mater. Res. A*, 2004, **69**, 525-534.
16. V. Vogel, *Annu. Rev. Physiol.*, 2018, **80**, 353-387.
17. G. Baneyx, L. Baugh and V. Vogel, *Proc. Nat. Acad. Sci. U. S. A.*, 2002, **99**, 5139-5143.
18. G. Baneyx, L. Baugh and V. Vogel, *Proc. Nat. Acad. Sci. U. S. A.*, 2001, **98**, 14464-14468.
19. E. Klotzsch, M. L. Smith, K. E. Kubow, S. Muntwyler, W. C. Little, F. Beyeler,

D. Gourdon, B. J. Nelson and V. Vogel, *Proc. Nat. Acad. Sci. U. S. A.*, 2009, **106**, 18267-18272.

20. S. Arnoldini, A. Moscaroli, M. Chabria, M. Hilbert, S. Hertig, R. Schibli, M. Behe and V. Vogel, *Nat. Commun.*, 2017, **8**, 1793.
21. K. E. Kubow, R. Vukmirovic, L. Zhe, E. Klotzsch, M. L. Smith, D. Gourdon, S. Luna and V. Vogel, *Nat. Commun.*, 2015, **6**, 8026.
22. W. C. Little, M. L. Smith, U. Ebneter and V. Vogel, *Matrix Biol.*, 2008, **27**, 451-461.
23. D. Ortiz Franyuti, M. Mitsi and V. Vogel, *Nano Lett.*, 2018, **18**, 15-25.
24. M. Chabria, S. Hertig, M. L. Smith and V. Vogel, *Nat. Commun.*, 2010, **1**, 135.